ELSEVIER

Journal of Nuclear Materials 279 (2000) 19–30

journal of nuclear materials

www.elsevier.nl/locate/jnucmat

On the recovery of the physical and mechanical properties of a CuCrZr alloy subjected to heat treatments simulating the thermal cycle of hot isostatic pressing

U. Holzwarth *, M. Pisoni, R. Scholz, H. Stamm, A. Volcan

European Commission, Joint Research Centre, Via E. Fermi 1 (T.P. 202), I-21020 Ispra (VA), Italy

Received 6 July 1999; accepted 28 November 1999

Abstract

Due to their high mechanical strength and thermal conductivity precipitation hardened CuCrZr alloys are being considered as potential heat sink material for the ITER divertor vertical target. The fabrication of the divertor component involves a joining procedure by hot isostatic pressing (HIP). The impact of this method on the degradation of the physical and mechanical properties of the CuCrZr alloy and their possible subsequent recovery by (re-)aging heat treatments have been investigated by hardness measurements, tensile testing and measurements of thermal diffusivity and electrical resistivity. The thermal cycle of hot isostatic pressing has been simulated by solution annealing finished by cooling rates between 0.03 and 1.5 K s^{-1}. The experiments revealed that a successful recovery of the desired mechanical strength is only achievable if cooling rates of about 1 K s^{-1} or higher can be realized after HIP. Otherwise the alloy becomes already over-aged during slow cooling after the joining procedure.

PACS: 28.52.Fa; 81.05.Bx; 81.40.Cd; 81.20.Vj

1. Introduction

Due to its high strength and high thermal conductivity CuCrZr alloys are being considered as heat sink material for the ITER divertor vertical target [1,2]. Compared with DS-copper the precipitation hardened CuCrZr alloy has some advantages, e.g., a better weldability and fracture toughness and more potential suppliers. The main problem to be solved is related to the thermal stability of this alloy under the joining procedures applied during divertor manufacture. The fabrication of divertor components involves a joining by hot isostatic pressing (HIP). Within the framework of ITER task T221 the HIP procedure was simulated by a solution annealing at 970°C for 20 min. Whereas solution annealing is usually finished by quenching in water, quenching cannot be applied for finishing hot isostatic pressing. In this case the component will cool in air or in an inert atmosphere. The cooling rate will therefore be much smaller and will exhibit local variations depending on the component geometry. A subsequent heat treatment has to be introduced in order to recover the initial mechanical properties of the precipitation hardened alloy and its physical properties, in particular the thermal conductivity.

The effect of various heat treatments simulating the thermal cycle of HIP and subsequent aging were characterized by hardness and thermal diffusivity measurements. The thermal diffusivity is directly related to the thermal conductivity of the alloy which is considered as the physical key property of the alloy to be applied as heat sink material. On the basis of these results a smaller number of heat treatments was selected for further investigation by tensile testing.

* Corresponding author. Tel.: +39-0332 785 194; fax: +39-0332 785 388.

E-mail address: uwe.holzwarth@jtc.it (U. Holzwarth).

0022-3115/00/$ - see front matter
PII: S0022-3115(99)00278-0

The paper is organized as follows. After the presentation of the heat treatment test matrix in Section 2.2, the results of the hardness measurements and the physical properties are presented in Sections 3.1 and 3.2, respectively. The latter contains also measurements of the electrical resistivity and a critical comment on the applicability of the Wiedemann–Franz law. Section 3.3 compiles the tensile properties of the alloy after selected heat treatment sequences.

2. Experimental procedures

2.1. Material

The CuCrZr alloy has been forwarded to Ispra by the ITER team, Garching in form of bars of $222 \times 54 \times 40$ mm^3 dimension cut from a cold rolled plate purchased from Zollern GmbH, Germany [3]. The chemical composition as certified by the supplier is given in Table 1 and satisfies the requirements for ITER grade CuCrZr alloys. The rolling direction was parallel to the longest side. After cold rolling the plate was solution annealed by holding a temperature of 970 ± 10°C for 20 min followed by quenching in cold water.

2.2. Heat treatments

The specimens were inserted in a quartz tube which was evacuated and then filled with high purity argon gas. Then the tube was inserted in a pre-heated tubular furnace such that the specimens were located within a zone of about 100 mm length in the centre of the furnace where a constant and homogeneous temperature was assured. The clock for the heat treatment was started when the desired temperature was reached. Furnace cooling was performed by switching off the furnace leaving the specimens in their position. Out-of-furnace cooling was realized by pulling the quartz tube out of the furnace. In both cases the quartz tube remained closed preserving the argon atmosphere.

A test matrix for the heat treatments was developed which contained the following seven treatments.

I. A solution annealing treatment, defined by the ITER team, at 970 ± 10°C for 20 min followed by water quench. Since the CuCrZr alloy was purchased in this solution annealed condition, it is further also referred to as the *as-received* condition. (This solution annealing followed by water quenching was not repeated in our examinations.)

II. A solution annealing treatment at 970 ± 10°C for 20 min followed by furnace cooling.

III. A solution annealing treatment at 970 ± 10°C for 20 min followed by out-of-furnace cooling.

IV. Aging treatment at 475°C for 3 h in argon gas atmosphere followed by furnace cooling.

V. Aging treatment at 425°C for 3 h in argon gas atmosphere followed by furnace cooling.

VI. Aging treatment at 525°C for 3 h in argon gas atmosphere followed by furnace cooling.

VII. Aging treatment at 475°C for 3 h in argon gas atmosphere followed by out-of-furnace cooling.

Treatments I to III define solution annealing treatments which were used to simulate the HIP procedure. They differ in the applied cooling rate when terminating solution annealing. Treatments IV to VII are aging treatments tested to recover the mechanical and physical properties. Treatment IV is the recommended aging treatment for this alloy to reach maximum mechanical strength. Treatments V and VI play with the aging temperature. They should give an indication how critical locally deviating temperatures may be to affect the result of aging. Treatment VII finally is the recommended aging treatment modified by applying a higher cooling rate. In order to check cooling rate effects on the efficiency to recover mechanical and physical properties by subsequent aging treatments a series of 15 heat treatment sequences labelled A to O were studied as illustrated in Table 2.

The cooling rates were determined using a small block of copper alloy with the dimension of $10 \times 12 \times 15$ mm^3 which was instrumented with a thermocouple type K inserted in a hole of 0.8 mm in diameter and 7 mm depth on the smallest face. The heating curve after inserting the quartz-tubes containing the instrumented specimen in the pre-heated tubular furnace and the cooling curves for furnace and out-of-furnace cooling were recorded and are presented in Fig. 1. The cooling curves are roughly characterized by a fast initial cooling phase when solution annealing ends, a critical cooling phase, when passing the temperature range in which aging effects take place, and a final phase of slow cooling. For cooling after solution annealing the temperature ranges for fast initial cooling and the criti-

Table 1
Chemical composition of the used CuCrZr alloy according to the supplier's certificate and the requirements for ITER grade CuCrZr alloy

Composition	Cu (wt%)	Cr (wt%)	Zr (wt%)	Impurities (wt%)
Present alloy	Balance	0.75	0.105	$P < 0.001$
ITER requirements	Balance	0.6–0.8	0.07–0.15	Total < 0.01; oxygen < 0.002

Table 2
Heat treatment test matrix[a]

Heat treatment	Heat treatment sequence														
	A	B	C	D	E	F	G	H	I	J	K	L	M	N	O
I (as-received)	×	×	×	×	×	×	×	×	×	×	×	×	×	×	×
II						×	×	×	×	×					
III											×	×	×	×	×
IV		×					×					×			
V			×					×					×		
VI				×					×					×	
VII					×					×					×

[a] The specimens were subjected to the heat treatments marked by ×, which are defined in Section 2.2. The table reads as follows: e.g., a specimen subjected to the heat treatment sequence H was received in the solution annealed condition I, then the solution annealing was repeated applying treatment II (with much lower cooling rate), subsequently the aging procedure V was applied.

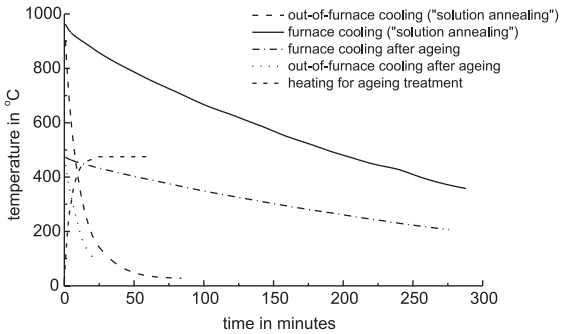

Fig. 1. Cooling curves for the applied heat treatments and heating curve for aging treatments.

cal cooling have been fixed between 970°C and 770°C and between 770°C and 370°C, respectively. Values of 0.06 and 0.03 K s^{-1} were obtained for the heat treatment II (furnace cooling) in the mentioned temperature ranges, respectively. Heat treatment III (out-of-furnace cooling) yielded values of 1.5 and 0.8 K s^{-1}, respectively.

In the case of the aging treatments IV and VII mean cooling rates were determined between 475°C and 300°C and between 300°C and 200°C. For the aging treatment IV with furnace cooling values of 0.02 and 0.014 K s^{-1}, respectively, were obtained. Treatment VII with faster out-of-furnace cooling yielded cooling rates of 0.5 and 0.3 K s^{-1}. Out-of-furnace cooling was found to be 20–30 times faster than furnace cooling.

2.3. Specimen preparation and experimental procedures

The screening of the effect of the heat treatments and heat treatment sequences on hardness was performed on blocks of CuCrZr alloy with dimensions of $10 \times 15 \times 20$ mm^3. The top face of the blocks was mechanically polished for improved visibility of microhardness indentations. All blocks were subjected to Vickers hardness measurements before and after the heat treatments according to the test matrix in Table 2. On several samples control measurements were performed after each heat treatment of the sequence.

The thermal diffusivity was measured by the laser flash method in transition [4] on two sets of round slabs of 2 mm thickness and 10 mm in diameter with polished surfaces. In order to check a possible influence of a preferential direction in the microstructure on the thermal diffusivity, the measurements were performed on two sets of slabs, which were cut parallel and perpendicular to rolling direction of the plate, respectively.

Electrical resistivity measurements were performed on thin stripes of the CuCrZr alloy with a cross-section of 0.25×1.4 mm^2 and 30 mm in length. They were produced by spark erosion and then electrolytically polished in order to remove the damaged surface layer and to obtain smooth and clean surfaces. The stripes were contacted by two spot welds in a distance of 21.2 mm.

Tensile tests were performed at room temperature, 200°C and 300°C in air on button headed specimens with a cylindrical gauge length of 20 mm and a diameter of 4 mm after selected heat treatments at a strain rate of 8×10^{-4} s^{-1}. The temperature variation along the gauge length and with time has been determined with a dummy specimen instrumented with three thermocouples and was $\Delta T \leqslant 1$ K. From load measurements and the controlled cross-head velocity stress–strain curves were derived and the yield stress at an offset of 0.2% plastic strain $\sigma_{0.2}$, the ultimate tensile strength σ_{UTS}, the uniform elongation ε_{UTS} and the elongation at fracture ε_{frac} were determined.

The tensile specimens were manufactured by machining in several runs with increasingly finer abrasion steps and fresh, sharp tools for the final machining runs. In this way a smooth and defect-free surface is obtained. Such a surface avoids the penetration of air into microcracks and tensile tests can reliably be performed at temperatures up to 300°C or even higher.

The specimens were named from A to O according to the heat treatment sequence they were subjected to.

3. Results

3.1. Micro- and macro-hardness

In Table 3 the mean values of the Vickers micro-hardness number HV 100 are compiled. Two sets of values are presented. The first set was obtained on the copper alloy blocks specified in Section 2.3 and the second one on the specimens prepared for the thermal diffusivity measurements. In order to check the sensitivity the micro-hardness measurements might exhibit due to local inhomogeneities of the microstructure additionally the Vickers HV 5 kg macro-hardness was measured. At least 5 micro- and macro-hardness indentations were taken for each condition. The micro- and macro-hardness numbers exhibit a statistical scatter of about ±5%. Comparing Tables 3 and 4 one recognizes that the micro- and macro-hardness numbers give identical results. In the as-received state (treatment I, first rows in Tables 3 and 4) the set of 15 specimens (A to O) exhibit some variability which is reflected both in the micro- and macro-hardness numbers. This indicates inhomogeneities on a macroscopic length scale, presumably caused by problems related to quenching of large, thick plates of CuCrZr. The supplier certifies a micro-hardness number of 64 in the as-received, solution annealed condition. This initial specimen variability vanished after performing the solution annealing treatments II or III, and the values obtained after aging treatment were not affected by the scatter in the as-received condition.

Micro-hardness numbers around 140, found in condition B after solution annealing finished by water quenching and the recommended aging treatment at 475°C for 3 h, may be considered as reference value for maximum micro-hardness. The slightly smaller values following from the aging treatments V and VI confirm that the aging temperature of 475°C is already optimized for the aging procedure.

One recognizes that the obtained micro-hardness numbers after aging fall roughly into two categories. The first category with Vickers micro-hardness numbers between 50 and 60 after the heat treatment sequences G to J and a second one with values ranging from over 90 to around 140 after the heat treatment sequences B to E and L to O. Although the same aging treatments were applied, the micro-hardness could not be recovered after solution annealing treatment II finished by slow furnace cooling. The ability of the CuCrZr alloy to recover the mechanical properties depends on the cooling rate after solution annealing. With regard to the divertor vertical target, this means that the mechanical properties cannot be recovered if the manufactured component is cooled too slowly after HIP. However, only moderate losses of the achievable micro-hardness after treatment III with a cooling rate of around 1 K s^{-1} are observed compared to treatment I finished by water quenching with typical cooling rates of some 10 K s^{-1}.

The somewhat higher micro-hardness values measured especially after the heat treatment sequences K to O on the small slabs prepared for thermal diffusivity measurements can be explained by the size effect, i.e., by faster cooling due to a higher surface-to-volume ratio.

The grain size has been determined in order to check a potential relation between grain size and micro-hardness. The grain size was determined using the linear intercept method. In the as-received condition (A) a grain size of 40 ± 10 μm was determined. The same value was obtained for the specimens B to E and K to O indicating that the applied heat treatments have a negligible influence on the grain size. The specimens F to J, however, exhibited a grain size between 90 and 140 μm. Grain growth was probably induced by the long holding times at elevated temperatures during slow furnace cooling. But the grain size cannot be responsible for the observed low hardness since the specimen in condition K with a grain size of about 40 μm exhibited the same micro-hardness numbers as the large-grained specimens. Moreover, after repeating the heat treatment sequences F to J, though the grains had grown to sizes of up to 240 μm, the micro-hardness numbers did not change. After subjecting the same specimens to the solution annealing treatment III and subsequently to the aging treatment IV, micro-hardness numbers between 110 and 120 were obtained which are consistent with the findings for the heat treatment sequence L. Thus, the effect of grain size on our findings can be excluded.

3.2. Physical properties

3.2.1. Thermal diffusivity

The thermal diffusivity was measured by the laser flash method in transition [4] on two sets of round slabs of 2 mm thickness and 10 mm in diameter with mechanically polished surfaces. Using a laser beam, a short heat pulse was produced on one side of the slab and the time-dependent temperature response was registered on the other side from which the thermal diffusivity can be derived [4,5]. The thermal diffusivity D_{th} is related with the thermal conductivity λ_{th} by

$$D_{\mathrm{th}} = \frac{\lambda_{\mathrm{th}}}{c_{\mathrm{p}} \varrho_{\mathrm{m}}}, \tag{1}$$

where $c_{\mathrm{p}} = 390$ J K^{-1} kg^{-1} [7,8] denotes the specific heat capacity at constant pressure and $\varrho_{\mathrm{m}} = 8.92$ g cm^{-3} [8] is the mass density of the material. The values given correspond to the values at 20°C.

Table 3
Synopsis of Vickers micro-hardness numbers (HV 100)[a]

Heat treatment	Heat treatment sequence														
	A	B	C	D	E	F	G	H	I	J	K	L	M	N	O
I (as-received)	70 68*	71	67	67	69	89	76	69	70	76	71	64	67	71	72
II						49 56*	×	×	×	×					
III											51 61*	×	×	×	×
IV		138 144*					55 59*					92 139*			
V			128 133*					53 60*					91 129*		
VI				122 127*					56 62*					98 125*	
VII					135 142*					55 62*					119 133*

[a] × indicates that the heat treatment was performed but no micro-hardness has been measured after this step. Values marked with * were obtained on round slabs of 2 mm thickness and 10 mm diameter. Each number is a mean value over 5 indents.

Table 4
Synopsis of macro-hardness measurements[a]

Heat treatment	Heat treatment sequence														
	A	B	C	D	E	F	G	H	I	J	K	L	M	N	O
I (as-received)	60 66*	62	59	57	58	×	×	×	×	×	×	×	×	×	×
II						42 51*	×	×	×	×					
III											49 53*	×	×	×	×
IV		138 –*					49 53*					105 131*			
V			128 –*					45 57*					103 124*		
VI				122 –*					49 57*					97 124*	
VII					135 –*					46 58*					113 132*

[a] All available Vickers HV 5 kg data are presented. × indicates the heat treatments were performed but no macro-hardness has been determined after this stage. Values marked with * were obtained from round slabs of 2 mm thickness and 10 mm diameter. Each number is a mean value over 5 indents.

Table 5 compiles the results of the thermal diffusivity measurements. In order to facilitate comparison with the hardness measurements we maintain the notations used in Tables 2–4.

No significant effect of the orientation of the slabs with respect to the rolling direction can be observed. Thermal diffusivity is lowest in the solution annealed condition (A) when chromium and zirconium atoms are expected to be in solid solution in the copper lattice. Precipitation during the aging treatments results in an increase in the thermal diffusivity by a factor of two. An increase is reasonable since the concentration of solid solution atoms in the copper lattice decreases when precipitates are formed under participation of the alloying elements. Thus, the concentration of scatter centers for phonons decreases.

In Fig. 2 the micro-hardness numbers are presented versus thermal diffusivity as measured on the slabs. One recognizes that all aging heat treatments lead to a nearly complete recovery of thermal diffusivity. But in the heat treatment sequences G to J the recovery of thermal diffusivity does not go along with the recovery of micro-hardness. After the solution annealing treatment II (condition F) the thermal diffusivity is already nearly as high as in the conditions B to E and L to O after the aging treatment. This indicates that the slow furnace cooling is equivalent to long holding times in the temperature range of aging. The formation of precipitates as indicated by the increased thermal diffusivity does not coincide with increased micro-hardness numbers. From this we conclude that the interparticle spacing increases as a result of coarsening of the precipitates. Thus, they are no longer effective in pinning dislocations and do not improve mechanical strength. This effect is known as over-aging and is obviously already brought about during furnace cooling. In the subsequent heat treatment the residual low concentration of solid solution atoms is further diminished which results in a further small increase in the thermal diffusivity but with no significant effect on the micro-hardness.

3.2.2. Electrical resistivity

Fig. 3 shows the change in electrical resistivity as a function of temperature measured for a cycle with increasing temperature between room temperature and 1000°C and reverse. The complete cycle as presented in Fig. 3 requires 24 h. The temperature changes were slow enough ($\leqslant 0.02$ K s^{-1}) to ensure resistivity measurements at practically constant temperature.

All measurements presented so far were performed at room temperature. This means that they belong to metastable quenched states established by (more or less) fast cooling. In Fig. 3, the measurements start with the specimen in the as-received condition (A). The electrical resistivity increases with temperature as expected for a metal. At around 370°C the resistivity starts to drop

Table 5
Thermal diffusivity in cm^2 s^{-1} measured by the laser flash method in transition[a]

Heat treatment	Heat treatment sequence															
	A	B	C	D	E	F	G	H	I	J	K	L	M	N	O
I (as-received)	*0.47*	×	×	×	×										
	0.47														
II						*0.85*	×	×	×	×					
						0.85									
III											*0.51*	×	×	×	×
											0.54				
IV		*0.90*					*0.89*					*0.91*			
		0.90					0.86					0.91			
V			*0.80*					*0.88*					*0.91*		
			0.85					0.86					0.91		
VI				*0.91*					*0.91*					*1.00*	
				0.96					0.94					1.01	
VII					*0.90*					*0.90*					*0.94*
					0.88					0.89					0.99

[a] The italicized numbers denote values for transition parallel to the rolling direction, the upright numbers for transition perpendicular to the rolling direction. The uncertainty is ±0.02 cm^2 s^{-1}.

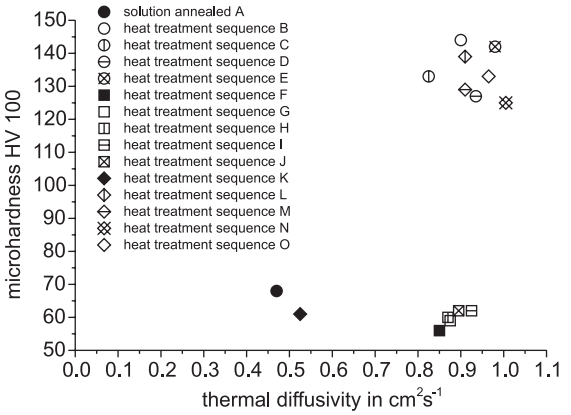

Fig. 2. The results of the micro-hardness measurements (HV 100) versus the corresponding thermal diffusivity measured on the same slabs after the heat treatment sequences A to O. The figures of the thermal diffusivity are the mean values of the pairs in Table 5 for transition parallel and perpendicular to the rolling direction.

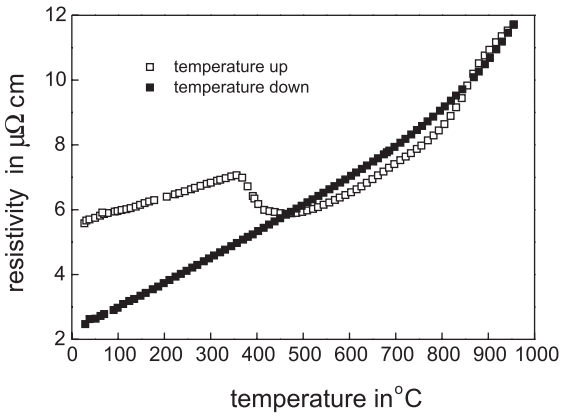

Fig. 3. Temperature dependence of the electrical resistivity of a thin CuCrZr plate initially in the as-received condition (A). For explanations see Section 3.2.2.

down and reaches nearly its initial room temperature value at 470°C. For further increase in temperature a monotonous increase of resistivity is observed up to the maximum temperature. During cooling down to room temperature a monotonous decrease of electrical resistivity is observed. The curve passes the minimum obtained on the heating branch and finally reaches a room temperature value which is roughly three times lower than the initial value. This indicates marked changes of the microstructure of the alloy during the thermal cycle performed in these measurements. In the notation of our heat treatments we identify the start of the measurements with the solution annealed and water quenched condition (A). After return to room temperature the material is expected to be in a condition similar to condition F, i.e., after slow furnace cooling from the solution annealing temperature to room temperature.

The resistivity drop observed during heating occurs in the temperature range between 370°C and 470°C which is the aging temperature range. The drop is likely to be caused by the formation of precipitates. The minimum refers to nearly complete precipitation and a minimum residual concentration of Cr and Zr atoms in solid solution of the copper lattice is achieved after about 1.5 h. The increase in the electrical resistivity after passing this minimum reflects the expected behaviour of metals and the more pronounced increase setting in around 750°C might be attributed to the onset of solution annealing and pronounced dissolution of precipitates. During slow cooling precipitates are formed and the concentration of solid solution atoms drops down to a minimum which is reflected in the low electrical resistivity after returning to room temperature.

The specific electrical resistivity of 1.678×10^{-6} Ω cm for elementary copper at 20°C is still about 50% lower than the value measured at the end of the thermal cycle in Fig. 3 but more than three times lower than in the solution annealed, initial condition.

The resistivity data reported above are consistent with those of Singh et al. [9]. Although they reported a resistivity in the solution annealed and quenched state which is about 35% lower than our value, the resitivity in a typical over-aged condition corresponds with ours in condition F. The deviation in the solution annealed state might originate from the lower solution annealing temperature applied by Singh et al. [9] (950°, 1 h). Thus, solution annealing might have been incomplete. Apart from their solution annealed state, these authors reported large variations (±20%) of the measured electrical resistivity after nominally equal heat treatments.

3.2.3. Considerations on the Wiedemann–Franz law

The contribution of electrons to the thermal conductivity λ dominates over the phonon contribution in a pure metal. The electrical conductivity σ_{el}, i.e., the inverse electrical resistivity $1/\varrho_{el}$, is determined by the scattering of electrons with phonons and with all crystal defects which disturb the crystal symmetry. Thus, for temperatures above the Debye temperature of the pure metal a relation between the electrical and thermal conductivity exists which reads

$$\frac{\lambda_{th}}{\sigma_{el}} = \frac{\pi^2 k_B^2}{3e^2} T \tag{2}$$

and is known as the Wiedemann–Franz law. Herein k_B denotes Boltzmann's constant and e the electron charge. Thus, for pure metals the so-called Lorenz number

$$\frac{\pi^2 k_B^2}{3e^2} = 2.45 \times 10^{-8}\ \mathrm{W\ \Omega\ K^{-2}} \tag{3}$$

is a universal constant. Below the Debye temperature Θ_D a lower value is expected since the thermal and electrical relaxation times become different towards lower temperature. The Debye temperature of pure copper is 315 K [6]. Although we cannot expect that the Wiedemann–Franz law is obeyed in our CuCrZr alloy, we may tentatively use the room temperature data of the electrical resistivity and of the thermal diffusivity in the state A and in the state F, which is assumed to be very similar to the situation at the end of the thermal cycle in Fig. 3. Under these circumstances we obtain for the constant (cf. Eq. (3)) values of 3.1×10^{-8} and 2.5×10^{-8} W Ω K^{-2} in the conditions A and F, respectively. We note, that both values have the right order of magnitude and that the value we ascribe to condition F is very close (2%) to the value expected for a pure metal. From the resistivity measured on the specimen subjected to the sequence E, 3.62 μΩ cm, and the corresponding value of the thermal diffusivity one gets 3.8×10^{-8} W Ω K^{-2}. This underlines that the Wiedemann–Franz law allows only a crude estimate of the electrical from the thermal conductivity and vice versa. A proportionality coefficient does not exist because the microstructures are different. From the different coefficients given above one concludes that estimates based on the Wiedemann–Franz law exhibit an uncertainty of up to 50%.

3.3. Tensile testing

Tensile tests were performed at constant cross-head velocity of 1 mm s^{-1} which corresponds to a strain rate of 8×10^{-4} s^{-1} at room temperature, 200°C and 300°C. The tests were performed on button headed cylindrical specimens with a gauge length of 20 mm and a diameter of 4 mm. A set of three specimens (A1 to A3) was tested in the as-received, solution annealed condition. 10 specimens (B1 to B10) were tested in condition B after being subjected to the recommended aging treatment IV. The tensile test results following from these specimens are considered as reference for maximum strength. A set of 10 specimens (G1 to G10) was tested in condition G in order to assess the deterioration of the mechanical properties in case of failure of the recovery treatment. The main emphasis was laid on the tensile properties after the heat sequences L (specimens L1 to L6) and O (O1 to O10) since these sequences are supposed to represent the most realistic simulation of HIP followed by aging.

The results are compiled in Fig. 4(a)–(d) and in Table 6. Since the $\sigma_{0.2}$ data were determined without applying extensometry, these data are only accurate within 10–15%. In the case of the specimens G1 to G10, which were extremely soft, the error margins are around 25% and the figures should be taken rather as a trend than as absolute values. The data for the ultimate tensile strength are correct within 1.5% and the elongation data within 4%.

From Fig. 4(a)–(d) it becomes evident that the heat treatment sequence O yields ultimate tensile stresses which are only 5–7% lower than our reference data obtained after the heat treatment sequence B. The treatment sequence L which differs only by the cooling rate when terminating the aging treatment results already in an ultimate tensile strength which is about 20% lower than those measured after the heat treatment sequences B and O. The mechanical strength after the heat treatment sequence G is even lower than in the solution annealed state A. The highest mechanical strength is related with the lowest values for uniform elongation and elongation at fracture.

For comparison the tensile properties certified by the supplier, Zollern GmbH, Germany [3], were included in Table 6 and Fig. 4. These data correspond to the microstructural condition after heat treatment sequence B. The yield point phenomenon which has been observed on specimen A2 was probably caused by some undesired cold-working during the manufacture of the tensile specimens. After subjecting them to any further heat treatment similar effects were not observed any more.

The specimens of Singh et al. [9] differ somewhat from ours because these authors performed the solution annealing treatment at 950°C for 1 h followed by water quench (here denoted as A′). This treatment was followed by aging at 475°C for only 30 min and terminated by water quenching (here denoted as B′). Thermal bonding was simulated by repeating treatment B′ an subsequent solution annealing at 950°C for 30 min followed by furnace cooling plus aging at 475°C for 30 min also followed by furnace cooling (denoted as G′). To G′ an over-aging treatment at 350°C for 100 h was added yielding to the condition denoted G″. Singh et al. as well as the supplier have chosen a test temperature of 250°C, thus at least the data of Zollern GmbH [3] can be expected to lay between our values obtained for 200°C and 300°C.

4. Discussion

The possible effects of the thermal cycle of hot isostatic pressing during manufacturing of the divertor vertical target and of subsequent aging treatments on the mechanical and physical properties of precipitation hardened CuCrZr alloy were investigated mainly by micro- and macro-hardness measurements, tensile testing and measurements of the thermal diffusivity. The degradation of the mechanical properties during hot isostatic pressing was simulated by solution annealing treatments with different final cooling rates. Subsequently, some aging treatments were tested to recover the desired materials properties.

Table 6
Results of the tensile testing for five sets of specimens, in the as-received condition (A) and after being subjected to the heat treatment sequences B, G, L and O[a]

Spec.	$\sigma_{0.2}$ (MPa)	σ_{UTS} (MPa)	ε_{UTS} (%)	ε_{frac} (%)
20°C				
$A1_l$	110	237	39.5	51
$B1_t$	273	355	15	23
$B2_l$	270	363	17.5	27
$G1_l$	37	227	50	60
$G2_t$	47	230	45.5	54.5
$L1_l$	164	315	28	39
$L2_t$	155	313	26.5	36
$O1_l$	255	382	18.5	27
$O2_t$	253	376	21	30
20°C (*supplier certificate*)				
B^+	311	423		25
200°C				
$A2_l$	145*	193	32.5	43
$B3_t$	248	300	14	25
$B4_t$	242	301	15	27
$B5_l$	256	303	13	22.5
$B6_l$	260	308	13.5	23
$G3_l$	27	175	47	56.5
$G4_l$	30	182	44.5	53
$G5_t$	35	173	41	48
$G6_t$	40	172	45.5	54
$L3_l$	146	254	24	33
$L4_l$	144	253	24.5	35
$L5_t$	144	252	23.5	34.5
$L6_t$	140	250	23	32.5
$O3_l$	230	309	16	22
$O4_t$	223	312	16.5	22
250°C (*supplier certificate*)				
B^+	300	383		23
300°C				
$A3_l$	110	191	27.5	36
$B7_t$	233	284	13	25.5
$B8_t$	223	272	13	24.5
$B9_l$	223	275	15.5	26.5
$B10_l$	240	278	10	18.5
$G7_l$	33	154	46	54.5
$G8_l$	31	151	45	53.5
$G9_t$	35	152	43	51
$G10_t$	37	153	43	52
$L7_l$	136	225	22.5	33
$L8_l$	138	228	24.5	36
$L9_t$	135	223	22.5	32
$L10_t$	133	226	21.5	32.5
$O5_l$	210	277	17.5	21
$O6_t$	208	277	16	21
250°C – Singh et al. [9]				
A'	56	177	33	36
B'	140	261	22.6	25.5
G'	100	219	27.3	31.3
G''	181	274	17.2	20.4

[a] The proof stress after 0.2% plastic strain $\sigma_{0.2}$, the ultimate tensile strength σ_{UTS}, the uniform elongation ε_{UTS} and the elongation at fracture ε_{fract} are presented. For comparison the data certified by the supplier are given which correspond to an aged condition similar to the present condition B, thus marked as B^+. The data of Singh et al. [9] belong to a solution annealed condition after 950°C for 1 h followed by water quench (A'). A' followed by aging at 475°C for 30 min and water quench leads to condition B'. Thermal bonding was simulated by repeating the heat treatment sequence B' and subsequent solution annealing at 950°C for 30 min finished by furnace cooling plus aging at 75°C for 30 min also followed by furnace cooling, here denoted as G'. To G' an over-aging treatment at 350°C for 100 h was added which led to the condition denoted G''. The tensile properties were determined at 250°C. * indicates a yield point phenomenon. The index l denotes specimens cut parallel to the rolling direction and t with the transverse direction. No significant effects due to the specimen orientation with respect to the rolling direction of the plate were observed.

The main result is highlighted in Fig. 2 where micro-hardness numbers HV 100 versus thermal diffusivity data are presented, which were obtained after various applied heat treatment sequences. From this we conclude that the thermal diffusivity can easily be recovered, whereas a recovery of the mechanical properties represented by the micro-hardness is only achievable if the solution annealing, i.e., the hot isostatic pressing is finished with a cooling rate of at least 1 K s^{-1}. Lower cooling rates are equivalent to long holding times in the temperature range of aging. The insufficient tensile properties indicate that the material is over-aged. Over-aging causes an increase in interparticle spacing due to the coarsening of precipitates. The most extreme case is observed after the heat treatment sequence G when the yield stress drops down to values around 40 MPa. In spite of the experimental uncertainty of this value, it is compatible with typical values obtained from zone-refined pure (99 999%) copper (58 MPa [10]) and on cold-rolled (≈80%) and annealed OHFC copper (63.5 MPa [11]). Over-aging is also confirmed by TEM and SEM investigations, which will be part of a forthcoming publication [12], which shows that only coarse precipitates with large interparticle distances in the range of 1–10 μm are present after heat treatment sequence G. Such precipitates are no longer effective in increasing strength

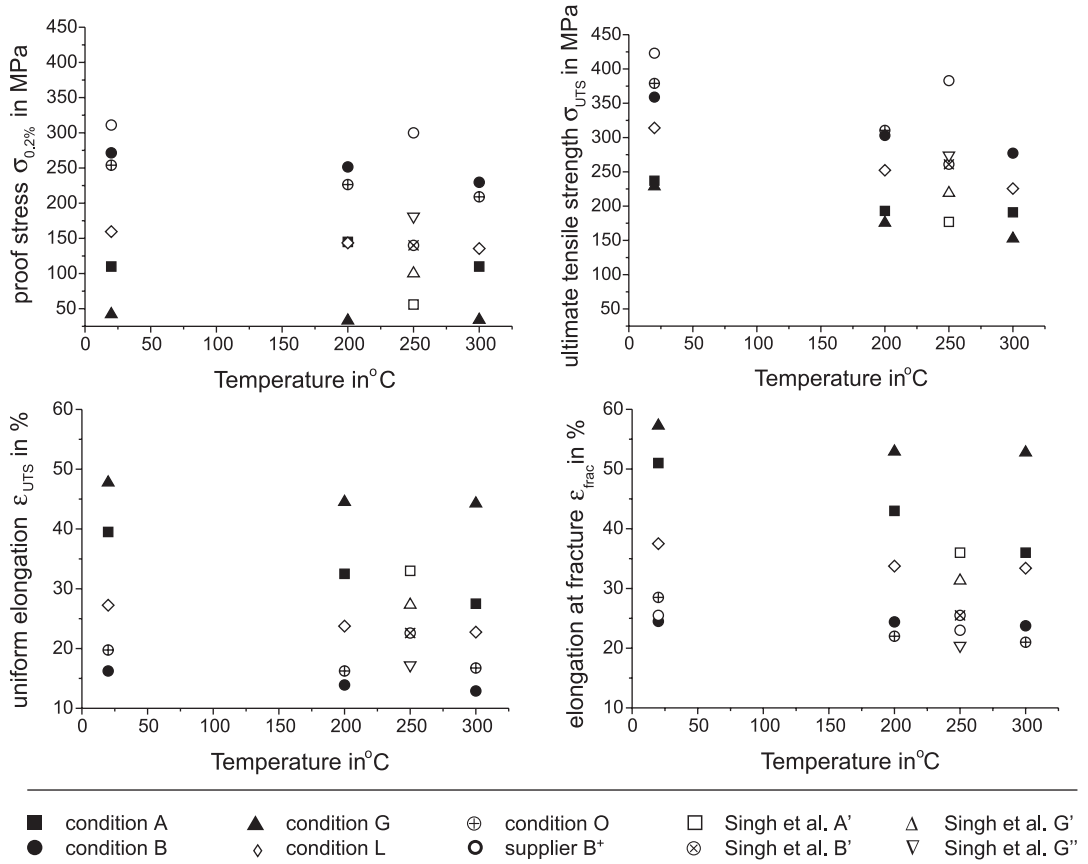

Fig. 4. Results of tensile testing, the proof stress at 0.2% plastic strain $\sigma_{0.2}$, the ultimate tensile strength σ_{UTS}, the uniform elongation ε_{UTS} and the elongation at fracture ε_{fract} for the as-received condition (A) and after the heat treatment sequences B, G, L and O. For comparison the test results of the supplier and the results obtained by Singh et al. [9] after similar heat treatments are included. For details see text and Table 6. (The figure presents the mean values of those given in Table 6 for certain heat treated conditions (where applicable).)

since the required Orowan stress becomes low because of the large spacing. Moreover, they concentrate the largest part of the alloying atoms. Therefore, the copper matrix is even softer than the one after heat treatment A when solution hardening is effective and yielding sets in at 110 MPa. (For comparison one should remember that the critical resolved shear stress of pure, well-annealed mono-crystalline copper is as low as about 1 MPa [13].) By alloying with Cr and Zr and cold-working prior to aging the room temperature yield stress of poly-crystalline CuCrZr may be shifted to over 500 MPa (e.g., [7]).

The yield stress and the ultimate tensile strength after the heat treatment sequence L are again about 20% lower than after the sequence O. The only difference between both treatments is the 20–30 times higher cooling rate when the aging treatment VII is applied instead of the recommended treatment IV ended by furnace cooling. The different tensile properties are also reflected in the micro-hardness numbers (cf. Table 3). Such a difference is not observed on the slabs for thermal diffusivity measurements which exhibit higher cooling rates due to their larger surface-to-volume ratio. Moreover, the micro-hardness values for slabs and blocks do not significantly differ in the case of the treatment sequences B to E and the values obtained in the cases B and E are identical within the error margins. From this we may draw two conclusions. Firstly, the higher the cooling rate after HIP the smaller are the problems in recovering the desired mechanical properties of the alloy. Secondly, after the heat treatment sequence O it was observed that a higher cooling rate after aging may also help to recover mechanical strength, provided that the cooling rate after hot isostatic pressing is not appreciably lower than about 1 K s^{-1}.

The data of Singh et al. [9] which are compiled in Table 6 and visualised in Fig. 4 for comparison underline the strong sensitivity of the mechanical properties to

details of the heat treatment. Although an influence of the slightly different composition of their alloy (0.8 wt% Cr, 0.07 wt% Zr and 0.01 wt% Si) cannot be excluded, it is still compatible with the ITER requirements according to Table 1. The main differences seem to be the applied heat treatments. A′ in Table 6 denotes a solution annealing at 950°C for 1 h followed by water quench. B″ is a sequence starting with A′ followed by aging for 30 min at 475°C, a HIP simulation by annealing at 950°C for 30 min followed by furnace cooling and subsequent re-aging at 475°C for 30 min also followed by furnace cooling. B″ denotes the treatment B″ plus a 100 h annealing at 350°C followed by furnace cooling. A comparison of the tensile test results shows the pronounced dependence on the details of the thermal treatments. In this light the higher strength specified by the supplier might be explained by higher obtained cooling rates due to furnace characteristics, a potential flow of protective gas or simply by specimen size effects.

Additionally, Singh et al. [9] point out that cold working prior to aging supports precipitation thereby increasing strength. A strong effect on the tensile characteristics due to cold-drawing between solution annealing and aging was also noted by Piatti and Boerman [7]. These authors found values for $\sigma_{0.2}$ and σ_{UTS} which are about 40% higher than the best values in the present work. The ratio $\sigma_{UTS}/\sigma_{0.2}$ ranges between 0.92 and 0.99 and indicates a small strain hardening capacity. Going along with the improved tensile strength a loss of ductility was found with values of ε_{UTS} and ε_{frac} below 7% and 19%, respectively. If effects of pre-deformation procedures shall be included in attempts to improve the mechanical properties of the CuCrZr alloy, the degree of deformation has to be adjusted to the maximum allowable service temperature. This is required by the fact that the higher the degree of deformation the lower is the temperature for the onset of recrystallization which will lead to a partial loss of mechanical strength [14].

The thermal diffusivity data in Table 5 and the tensile properties compiled in Table 6 show that the conclusions to be drawn from the thermal diffusivity with respect to the tensile strength are limited. Only solution annealed states (A and K) are discernible from other states with pronounced precipitation. The quality of precipitation, i.e., if properly aged or over-aged, cannot be distinguished. Thermal and electrical conductivity are sensitive to the concentration of alloying atoms in solid solution in the copper matrix. Precipitation reduces this concentration but the sensitivity is not sufficient to further distinguish between fine and coarse precipitates and their respective densities. Nevertheless, non-destructive photothermal measuring techniques [4] may be applied to check whether or not the alloy is still in the solution annealed state after hot isostatic pressing and therefore susceptible to a subsequent aging treatment. For this purpose it seems to be sufficient to distinguish between thermal diffusivity values of 0.5 ± 0.05 cm^2 s^{-1} (solution annealed) and 0.95 ± 0.05 cm^2 s^{-1} (over-aged if measured immediately after HIP). An over-aged precipitation structure could only be cured by a further solution annealing of the hole component finished with sufficiently high cooling rate.

Although the Wiedemann–Franz law does not allow a quantitative translation of thermal into electrical conductivity data and vice versa in an alloy, it is clear that the principle problems described in the preceding paragraph for thermal diffusivity data exist in the same way for the electrical resistivity. This is reflected in the resistivity values reported by Singh et al. [9] measured after different heat treatments. Quantitative agreement with the values in the present work exists for the over-aged state when the value is close to the one of pure copper. The resistivity isochrone presented in Fig. 3 shows the way to investigate the precipitation kinetics. Isothermal measurements might be applied to determine the kinetics of annealing and precipitation. If the service temperature of the alloy may temporarily exceed 350°C, data on the precipitation kinetics would be helpful in order to estimate the rate of degradation of mechanical properties and to calculate tolerable holding times.

A further effect on the microstructure may arise due to the effect of the high pressure of typically 100–120 MPa. There is little known on the combined effect of pressure and high temperature on the diffusion behaviour of chromium in copper, which may influence the precipitation kinetics. However, this will affect more the dissolution of the precipitates when holding high temperature and pressure for HIP than the deleterious effects of over-aging when slowly passing the temperature range of aging after the joining procedure when the load is already removed.

5. Conclusions

The necessity for high cooling rates to terminate the hot isostatic pressing procedure poses a challenge for the manufacturing of the divertor vertical target using CuCrZr alloy. Since quenching of the whole component after joining is not feasible, cooling should at least be supported by a cold gas stream. This is even more important if the alloy is joint with stainless steel which exhibits a low thermal conductivity. Alternative HIP procedures working at lower temperature should also be considered [15] if they may help to reduce the effective holding time in the critical temperature range in which the risk of over-aging exists. Moreover, the processing of the alloy before joining may still be optimized, e.g., by paying more attention to the degree of pre-deformation of the alloy. Although CuCrZr is a commercially available alloy there is a lack of knowledge concerning the

precipitation kinetics and the type of precipitates. A better understanding would allow a more reliable assessment of the effect of holding times and cooling rates after thermal treatments as well as tolerable service parameters.

Acknowledgements

The authors thank S. Colpo, A. Pisoni, and M. Airola for their technical assistance in metallography and mechanical testing.

References

[1] ITER Joint Central Team, J. Nucl. Mater. 212–215 (1994) 3.
[2] J.W. Davies, D.E. Driemeyer, J.R. Haines, R.T. McGrath, J. Nucl. Mater. 212–215 (1994) 1352.
[3] Zollern GmbH, Germany, Certificate No 1754/91, Heat No. 822, Test specimen No. 22.
[4] L. Fabbri, P. Fenici, Rev. Sci. Instrum. 66 (1995) 3593.
[5] BS 7134: Section 4.2 – 1990 Testing of engineering ceramics, Section 4.2 – Method for the determination of thermal diffusivity by the laser flash or heat pulse method, British Standard Institution, 1990.
[6] N.W. Ashcroft, N.D. Mermin, Solid State Physics, Saunders, Philadelphia, PA, 1976.
[7] G. Piatti, D. Boerman, J. Nucl. Mater. 185 (1991) 29.
[8] Handbook of Chemistry and Physics, 40th Ed., Chemical Rubber, Cleveland, OH, 1958/1959, p. 2265.
[9] B.N. Singh, D.J. Edwards, M. Eldrup, P. Toft, J. Nucl. Mater. 249 (1997) 1.
[10] H.R. Brager, H.L. Heinisch, F.A. Garner, J. Nucl. Mater. 133&134 (1985) 676.
[11] B.N. Singh, D.J. Edwards, P. Toft, J. Nucl. Mater. 238 (1996) 244.
[12] U. Holzwarth, H. Stamm, this issue, p. 31.
[13] J. Diehl, R. Berner, Z. Metallkd. 51 (1960) 522.
[14] R.W. Cahn, in: R.W. Cahn, P. Haasen (Eds.), Physical Metallurgy, vol. 2, North-Holland, Amsterdam, 1984, p. 1506.
[15] F. Saint-Antonin, D. Barberi, G. LeMarois, A. Laillé, in: C. Varandas, F. Serra (Eds.), Proceedings of the 19th Symposium on Fusion Technology, 16–20 September 1996, Lisbon, Portugal, Elsevier, Amsterdam, 1997, p. 399.